Journal of Molecular Modeling (2022) 28: 68
https://doi.org/10.1007/s00894-022-05056-4

ORIGINAL PAPER

Antiradical properties of curcumin, caffeic acid phenethyl ester, and chicoric acid: a DFT study

Brenda Manzanilla[1] · **Juvencio Robles**[1]

Received: 5 August 2021 / Accepted: 11 February 2022 / Published online: 26 February 2022

Abstract

The antiradical properties and possible mechanisms of action of the tautomers of curcumin, caffeic acid phenethyl ester (CAPE), and chicoric acid (CA) have been studied within density functional theory (DFT). We calculated global chemical reactivity descriptors from conceptual DFT, pK_a, bioavailability, and toxicity to evaluate the antiradical properties and characterize these species. Our final level of theory is the M06-2X functional with the 6–31 + G* basis set; we selected this level after performing a benchmark calibration and validation among different levels. Solvent effects were modeled via the continuum solvation model based on density (SMD). We used water and pentyl ethanoate as solvents to simulate the physiological conditions. The free radical scavenger capacity was analyzed for three possible oxidative stress mechanisms: single electron transfer (SET), hydrogen atom transfer (HAT), and xanthine oxidase (XO) inhibition. The results indicate that neutral curcumin, CA, and CAPE behave as antireductants. The most favorable mechanism turns out to be HAT, where CA and CAPE stand out. In conclusion, our DFT study strongly indicates that neutral curcumin, CAPE, and CA would very likely perform well as antiradical drugs with recommended therapeutic use, supported by their non-toxic nature.

Keywords Antiradical properties · Conceptual DFT · Chicoric acid · Curcumin · Caffeic acid phenethyl ester · ADME

Introduction

Oxidative stress, a disturbance in the prooxidant-antioxidant balance, is associated with the pathogenesis of many diseases associated with radical damage, including neurodegenerative diseases (Alzheimer's disease and Parkinson's disease), several types of diabetes, cardiovascular diseases, cancer, etc. [1]. Oxidative stress is associated with high levels of the so-called reactive species such as reactive oxygen (ROS), reactive nitrogen (RNS), and reactive sulfur species (RSS), namely free radicals (FR). The overproduction of FR may result in DNA, lipid, and protein damage [2]. Antiradical (AR) molecules can interact with FR and terminate their chain reaction by different mechanisms [3].

AR prevent radical damage by an oxidation mechanism or a reduction mechanism of FR [4]. The mechanisms of AR are primary, chain-breaking, by forming stable FR. In secondary mechanisms, preventive antiradicals do not involve direct reactions with FR and do not convert them to more stable products. Finally, tertiary mechanisms fix damaged biomolecules [5]. Moreover, some ARs may exhibit more than one mechanism; they are classified as multifunctional antiradicals. AR exist in different sources: endogenous (enzymatic or nonenzymatic compounds in the human body) and exogenous (compounds in fruits, vegetables, and plants) [6]. The effort of research groups devoted to finding chemical compounds with antiradical properties to prevent radical damage is well documented [7–9].

Several research groups have performed theoretical studies to explore mechanisms and antiradical properties of certain molecules to suggest new AR [10–16]. Such is the case of exogenous molecules produced by some plants such as lycopene, a red carotenoid present in tomatoes, watermelon, guava, etc. [14]; silybin, a medicinal plant [16]; curcumin, a yellow-orange pigment derived from the rhizome of *Curcuma longa* [17]; and vitamins such as vitamin C and vitamin A [18, 19]. These studies show different possible mechanisms as primary mechanisms: single electron transfer (SET) and hydrogen atom transfer (HAT). Altogether, the results describe structural properties that are important for

✉ Juvencio Robles
roblesj@ugto.mx

[1] Departamento de Farmacia, DCNE, Universidad de Guanajuato, Noria Alta S/N. Col. Noria Alta, Gto. C. P. 36050 Guanajuato, México

antiradical activity. In addition, these properties help against FR. As a result, they show that some exogenous molecules can be good AR.

Some recent experimental and theoretical studies of exogenous molecules suggest that they can be good antioxidants. These molecules are curcumin [20]; chicoric acid (CA), a caffeic acid derivative present in *Echinacea purpurea* and basil leaves (*Ocimum basilicum*) [21, 22]; and caffeic acid phenethyl ester (CAPE), a polyphenolic chemical compound present in the *apiproduct propolis*, obtained from beehives [23]. These studies suggest that curcumin, CA, and CAPE are good antioxidants; however, their mechanism of action and their antiradical properties are still not well known. In this work, we show how to characterize them and whether they are good AR. For this purpose, we examine the antiradical properties and mechanisms of action of curcumin, CA, and CAPE. We use vitamin A and E as controls. We obtain reactivity properties, log *P*, solvation free energy, bioavailability, and toxicity using density functional theory (DFT).

We examine curcumin, both tautomers of curcumin (keto-enol curcumin (CKE) and diketone curcumin (CDK)), CA, CAPE, vitamin A, and vitamin E, (structures in Fig. 1). Moreover, we use Conceptual Density Functional Theory (CDFT) [24], to compute the global chemical descriptors of reactivity. Furthermore, we study three possible oxidative stress mechanisms: SET, HAT, and xanthine oxidase (XO) inhibition; the latter is an enzyme that generates reactive oxygen species [25]. Moreover, to locate the specific atoms in the molecule that can donate or accept electrons from FR, we use the local ionization potential map and the LUMO map.

Benchmark and computational details

All electronic calculations were performed with the Gaussian 09 package [26]. Local minima were identified by the absence of imaginary frequencies. A small benchmark study comparing several DFT methods was carried out to validate the chosen computational procedure selected for the best cost/performance compromise. Eight levels of theory (B3LYP/6–31 + G*, B3LYP/6-311G**, B3LYP/6–311 + G**, M06-L/6-31G*, M06-L/6–31 + G*, M06/6–31 + G*, LC-ωPBE/6–31 + G*, and

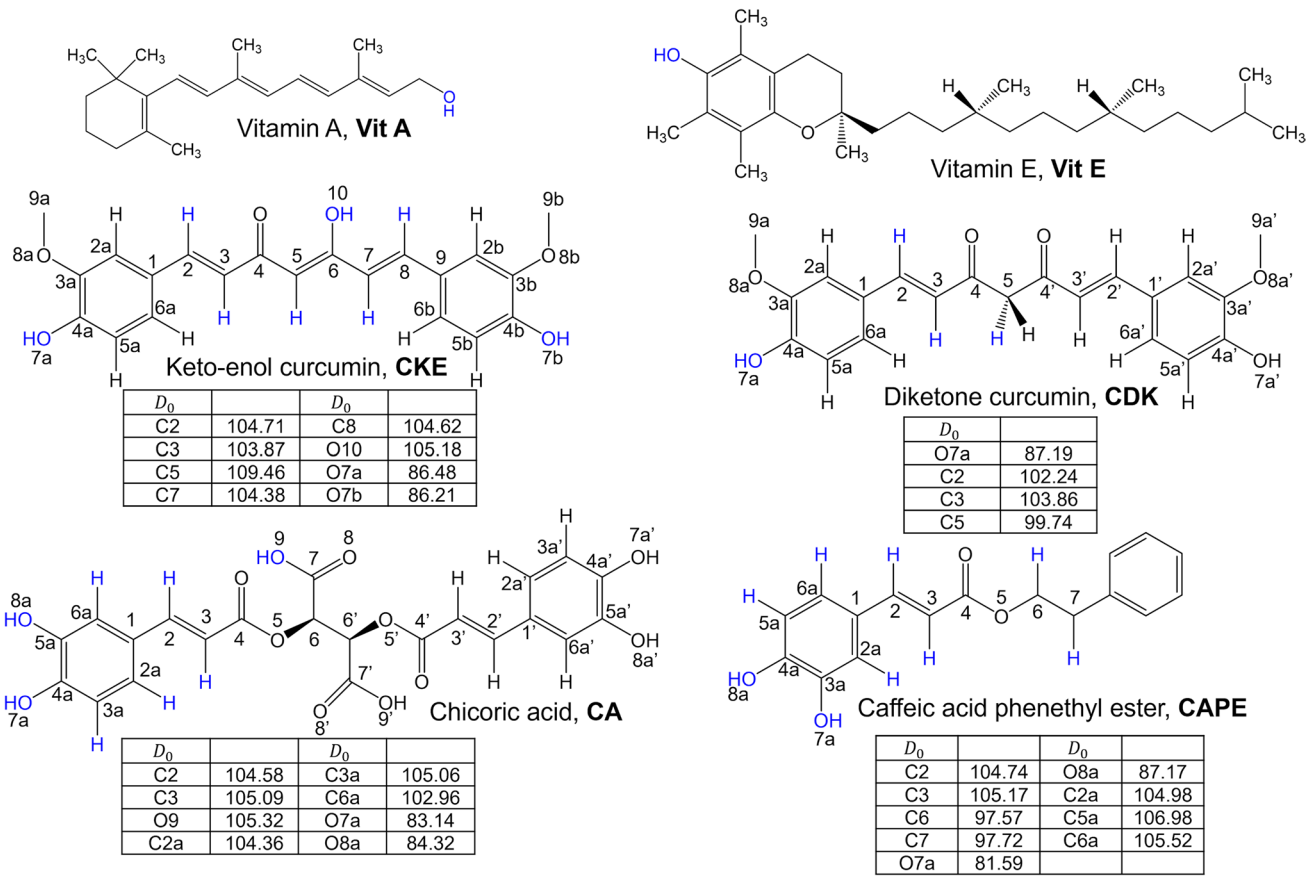

D_0		D_0	
C2	104.71	C8	104.62
C3	103.87	O10	105.18
C5	109.46	O7a	86.48
C7	104.38	O7b	86.21

D_0	
O7a	87.19
C2	102.24
C3	103.86
C5	99.74

D_0		D_0	
C2	104.58	C3a	105.06
C3	105.09	C6a	102.96
O9	105.32	O7a	83.14
C2a	104.36	O8a	84.32

D_0		D_0	
C2	104.74	O8a	87.17
C3	105.17	C2a	104.98
C6	97.57	C5a	106.98
C7	97.72	C6a	105.52
O7a	81.59		

Fig. 1 Chemical structures of the antiradicals studied in this work. In blue color, H atoms selected for dehydrogenation studies, and the calculated energy of the related reaction, D_0, values in kcal/mol

M06-2X/6–31 + G*) were employed to compute the vertical ionization energy (*I*) of Vit A, used as control. The calculated *I* values were compared with the experimental value, 6.95 eV, for Vit A [27]. In addition, we compared the computational time for Vit E and Vit A in every level of theory. The continuum solvation model based on density (SMD) [28] was used to include solvent effects of water (ε = 78.36) and pentyl ethanoate (ε = 4.73), chosen to mimic aqueous and lipid environments.

Conformational search

We performed a conformational search in Spartan 08 [29]. The utility "conformer distribution" was employed with the MMFF force field [30–33]. We restrict the search to 10,000 conformers, to obtain the 10 lower energy final conformers without imposing any symmetry restrictions. These 10 conformers were reoptimized at the B3LYP/6–31 + G* level of theory. Finally, we selected the minima energy conformers for each molecule studied and reoptimized with M06-2X/6–31 + G* level of theory.

pK_a calculation

To mimic any molecule under physiological conditions (aqueous phase), it is important to know which would be the prevailing acid/base form. To that end, it is necessary to know the pK_a value which is many times not known experimentally. Therefore, we estimated the pK_a value of all the AR under study using the proton-exchange scheme [34]. In this work, we used the so-called direct method, cycle A below,

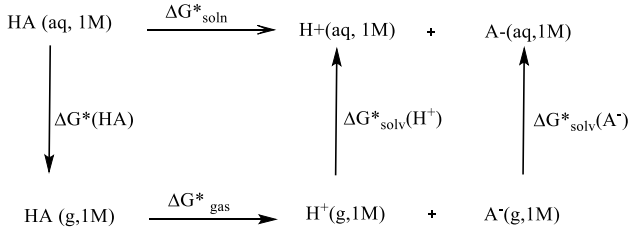

Scheme 1 pK_a calculation via the direct method

with the following equations,

$$AH_{aq} \rightarrow A^-_{aq} + H^+_{aq} \tag{1}$$

$$pK_a = \frac{\Delta G^*_{soln}}{RTln(10)} \tag{2}$$

$$\Delta G^*_{soln} = \Delta G^*_{gas} + \sum_{i=1}^{N\ products} n_i \Delta G^*_{solv,i} - \sum_{j=1}^{N\ reactants} n_j \Delta G^*_{solv,j} \tag{3}$$

Some needed values were taken from the work of Coote, M. L. [34].

Global descriptors

To understand the reactivity of our molecules towards the FR, we employed the following reactivity global descriptors of CDFT [24]. Electronegativity (χ) measures the electrons tendency to escape from the system. χ is obtained by a finite differences approximation [35] as follows:

$$\chi = \frac{I + A}{2} \tag{4}$$

where the vertical ionization energy (*I*) and electron affinity (*A*) have been used. *I* measures the vertical energy required to remove an electron from the neutral system ground state. *A* measures the vertical energy when a neutral system in its ground state captures one electron [36, 37]. *I* and *A* are calculated as follows:

$$I = E(N-1) - E(N) \tag{5}$$

$$A = E(N) - E(N+1) \tag{6}$$

It is necessary to compute single point energies of the cationic $(N-1)$ and anionic $(N+1)$ molecules at the optimized neutral structure.

Chemical hardness (η) measures the resistance of a molecule to intramolecular charge transfer. η indicates the reactivity of the molecule [38, 39]. η is calculated as follows:

$$\eta = I - A \tag{7}$$

Electrophilicity index (ω) measures the stabilization energy when a system attracts electronic charge [40]. To measure the response of the system for the addition and/or removal of charge, it developed the electrodonating power index (ω^-) and the electroaccepting power index (ω^+) [41]. ω^- measures the capability of the system to donate a fractional amount of charge and ω^+ measures the capability of the system to accept charge. ω^- and ω^+ can be approximated as follows [41]:

$$\omega \equiv \frac{(I+A)^2}{8(I-A)} \tag{8}$$

$$\omega^+ \equiv \frac{(I+3A)^2}{16(I-A)} \tag{9}$$

$$\omega^{-} \equiv \frac{(3I + A)^2}{16(I - A)} \tag{10}$$

Solvation free energy and log *P*

Solvation free energy (ΔG°_{solv}) is a property useful for the thermodynamical description of a solution. ΔG°_{solv} describes the relative stability of a chemical species in the solution concerning the gas phase at equilibrium. As a result, ΔG°_{solv} indicates the preference of one phase over the other [42]. The solvation energies were obtained as follows:

$$\Delta G^{\circ}_{solv} = G_{solvent} - G_{gas} \tag{11}$$

Then, it was necessary to compute the Gibbs free energies of the optimized structure in gas (G_{gas}), water, and pentyl ethanoate ($G_{solvent}$).

Whereas the log *P* value is the octanol/water partition coefficient, which is traditionally used to assess the hydrophobicity of compounds and estimate their membrane permeability [43]. Log *P* value was calculated for every optimized structure in Spartan 18 [44] with the utility QSAR. Log *P* was calculated using predictions based on quantitative structure relationships (QSAR) of Ghose, Pritchet, and Crippen [45].

Bioavailability, ADME properties, and toxicity

Lipinski's rules [46], Ghose's rules [47], and Veber's criteria [48] provide empirical values of properties useful to assess the drug's pharmacokinetics in the human body, such as absorption, distribution, metabolism, and excretion (ADME). These rules determine if a molecule is likely to perform well as an orally active drug in humans. Lipinski's rules state that drugs should have no more than 5 hydrogen bond donors (HBD), no more than 10 hydrogen bond acceptors (HBA), a molecular weight (MW) under 500 amu, a log *P* value lower than 5. On the other hand, Ghose's rules state that drugs should have a log *P* value from − 0.4 to 5.6, molar refractivity (AMR) from 40 to 130 m^3mol^{-1}, MW from 160 to 480 amu, and the number of atoms from 20 to 70 (nAtom). Finally, the Veber's criteria establish that the successful drugs should have no more than 10 rotable bonds (nRB), no more than 12 HBD, and a polar surface area (PSA) equal to or less than 140 $Å^2$. Molecules that violate more than one rule may have problems with bioavailability. Our molecules' ADME values were obtained using DruLiTo software [49].

We used the Toxicity Estimations Software Tool (T.E.S.T) to investigate the toxicity [50]. This program makes its predictions using quantitative structure–activity relationships (QSAR). The descriptors computed in this way were the median lethal dose (LD_{50}) and the mutagenicity (M). LD_{50} is the amount of material (mg/kg), which causes the death of 50% of rats after oral ingestion. M, known as Ames test, is a bacterial bioassay to evaluate the mutagenicity caused on the DNA of *Salmonella typhimurium*.

Single electron transfer

To investigate the SET mechanism, Eq. 12, we used two graphical strategies. The full-electron donor–acceptor maps (FEDAM) is employed to evaluate and characterize the electron-transfer process between AR and FR. FEDAM graphs *I versus A*. Thus, FEDAM provides information about electron-donor and electron-acceptor behaviors of a given molecule [51]. In this research, we worked with the following FR: $OH^{\cdot}$, $NO_2^{\cdot}$, $HOO^{\cdot}$, and $CH_3O^{\cdot}$. These FRs were selected as representative of FRs containing oxygen, carbon, and nitrogen. The donator-acceptor map (DAM) classifies a molecule in terms of its electron donating-accepting capacity [52]. DAM is useful when comparing different molecules; they can be classified according to their electron donating-accepting capacity relative to F and Na. Then, it is necessary to graph the electron acceptance (*Ra*) *versus* the electron donation index (*Rd*), defined by Eqs. 13 and 14.

$$AR + FR^{\cdot} \rightarrow AR^{\cdot +} + FR^{-} \tag{12}$$

$$Ra = \frac{\omega_L^+}{\omega_F^+} \tag{13}$$

$$Rd = \frac{\omega_L^-}{\omega_{Na}^-} \tag{14}$$

Hydrogen atom transfer

Another possible mechanism for scavenging FR is HAT, represented as follows:

$$AR + FR^{\cdot} \rightarrow AR^{\cdot}_{(-H)} + FRH \tag{15}$$

For HAT, we also studied the dissociation energy of one hydrogen atom within the molecule (D_0).

$$D_0 \equiv AR \rightarrow AR^{\cdot}_{(-H)} + H^{\cdot} \tag{16}$$

We computed the adiabatic Gibbs free energy for all reactions. We evaluated the antiradical action of all molecules under study with the following FRs: $OH^{\cdot}$, $NO_2^{\cdot}$, $HOO^{\cdot}$, and $CH_3O^{\cdot}$.

Inhibition of xanthine oxidase

Docking studies were based on the X-ray structure of *Bos Taurus* (90% homology with human XO) at 2.5 Å resolution when forming a complex with its competitive inhibitor salicylic acid (SAL), with PDB code: 1FIQ [53]. XO and ligands docking studies were performed with AutoDock Tools package version 1.5.6 and AutoDock 4.2.6 [54]. To merge nonpolar hydrogens, we calculated Kollman charges. We removed A and B chains of the protein and small molecules except molybdopterin cofactor (MTE) and Mo cofactor (MOS) in the C subunit of the protein. We used grids for docking evaluation with a spacing of 0.375 Å and 40 × 40 × 60 points centered in 26.569 × 10.228 × 113.088 with a Lamarckian Genetic Algorithm [55]. We performed flexible Docking studies. We selected the following residues as flexible: LEU873, LEU648, GLU802, SER876, ARG880, PHE914, PHE1009, THR1010, VAL1011, LEU1014, ALA1079, and GLU1261 where GLU802, THR1010, ARG880, PHE914, PHE1009, LEU873, VAL1011, and LEU648 are catalytic residues and GLU802, GLU1261, and ARG880 play key roles in the hydroxylation of substrate xanthine [56]. All molecular graphics material was prepared using the Discovery Studio 2017 R2 Client (ver. 17.2.0, Accelrys Software Inc., San Diego, CA, USA).

Results and discussion

To select a reliable level of theory, we tested the following levels: B3LYP/6–31 + G*, B3LYP/6-311G**, B3LYP/6–311 + G**, M06-L/6-31G*, M06-L/6–31 + G*, M06/6–31 + G*, LC-ωPBE/6–31 + G*, and M06-2X/6–31 + G*. These were chosen because they represent a variety of the most employed levels of theory in other works and some were selected by their low computational cost. We compared the absolute error between calculated *I* and experimental *I* (Table 1), computational time, and global descriptors; see Figs. S1 and S2 in the supporting information. According to the computational times, with B3LYP, M06-L, and M06-2X functionals and small basis sets, it is less expensive to obtain optimization and frequencies calculations (Fig. S1). We compared computed values of some global descriptors: I, η, ω, and ω^- at various levels of theory, finding low variation in the values. The range percent values are for I 14%, for ω^- 12%, for η 18%, and for ω 14% (Fig S2). Finally, according to Table 1, M06-2X/6–31 + G* yields the smallest absolute error; therefore, it was selected to perform all the forthcoming studies, since it exhibits the best cost/performance compromise.

Table 1 Vit A vertical ionization energy calculated in eV at different levels of theory and % absolute error between calculated *I* and experimental *I* value

Level of theory	*I*	% error
Vit A		
B3LYP/6–31 + G**	6.60	5.0
B3LYP/6-311G**	6.61	4.9
B3LYP/6–311 + G*	6.68	3.9
M06-L/6-31G*	6.23	10.3
M06-L/6–31 + G*	6.35	8.6
M06/6–31 + G*	6.66	4.1
LC-ωPBE/6–31 + G*	7.22	3.9
M06-2X/6–31 + G*	7.08	1.9
Exp	6.95	0.0

Conformational search

We used the optimized geometry at the global minimum and the closest conformers found at local minima to examine the global reactivity descriptors, but only the global minimum conformer was used in the other studies. First, at the B3LYP/6–31 + G* level of theory, we selected the conformers closest to the global minimum conformer within a difference of ~ 0.6 kcal/mol. Thereafter, these conformers were reoptimized at the M06-2X/6–31 + G* selected level of theory. Furthermore, we used the root mean square deviation (RMSD, Eq. 17) for dihedral angles to compare the closest conformers with the global minimum conformer; see Fig. S3.

$$RMSD = \sqrt{\frac{1}{N}\sum_{i=1}^{N}\left(X_{i,test} - X_{i,global}\right)^2} \tag{17}$$

where N is the number of dihedral angles tested, X_{test} is the value of the dihedral angle in the tested conformer, and X_{global} is the value of the same dihedral angle in the reference global minimum conformer. As a result, we only found different conformers for Vit A, CDK, and CAPE. For CKE, CA, and Vit E, we only have the global minimum conformer. CA has an asymmetric carbon; our structure is the L-chicoric acid ((2R,3R)-2,3-bis[[(E)-3-(3,4-dihydroxyphenyl)prop-2-enoyl]oxy]butanedioic acid). Our CA optimized molecule is a V-shaped conformation with large separation between the tail-ends, with no hydrogen bonds. Nobela et al. have reported that the RR conformation is the most stable due to hydrogen bond interactions [57]. This conformer was obtained by molecular dynamics calculations with the AmberTools algorithm. Its conformer has several internal hydrogen bonds and is not V-shaped, so it is very different from ours.

Table 2 First pK_a values and molar fraction calculated from the neutral ($mf_{neutral}$) and anionic (mf_{anion}) species at pH = 7.4 for Vit A, Vit E, CKE, CDK, CA, and CAPE at 1 M standard state

Molecule	pK_a	$mf_{neutral}$	mf_{anion}
Vit A	21.9	1.00	0.00
Vit E	15.0	1.00	0.00
CKE	8.7	0.95	0.05
CDK	8.3	0.89	0.11
CA	8.4	0.90	0.10
CAPE	8.2	0.86	0.14

For Vit A, we found two conformers with an RMSD value of 127.19°. The difference between conformers of Vit A is in the alkyl chain. For CDK, there are three conformers. Conformer 2 has an RMSD value of 229.18° and conformer 3 of 74.48°; they exhibit several geometry changes in the orientation of the methoxy group and the keto groups in the hepta-1,6-diene-3,5-dione structure. For CAPE, there are three different conformers. Conformer 2 has an RMSD value of 149.54° and conformer 3 of 87.08°. The principal changes observed correspond to orientation possibilities of the phenyl group; these are more significant for conformer 2. We found that conformer CKE is like the one found by Galano et al., and in the same work, they report our second CDK conformer as the minimum [17]. The second CDK conformer has an energy difference with the minimum of 0.001 kcal/mol which is very small. On the other hand, Singh et al. [58] and Puglisi et al. [59] report similar conformers with the B3LYP/6–31 + g(d, p) level of theory and molecular dynamics.

pK_a calculation

According to our computed pK_a values (Table 2) at physiological pH (7.4), all the molecules are in neutral form. Therefore, the neutral form was used in this work to study the free radical scavenging activity. To assess which H is involved in the deprotonation mechanism, we chose H atoms from -NH, -NH_2, -COOH, and -OH groups. For Vit A, we studied the hydrogen in the -OH group and for Vit E, the hydrogen at -OH group. For CDK, we selected hydrogens H7a and H7a' at -OH groups (Fig. 1). For CKE, according to the lower D_0 value in Fig. 1, we selected H7b from the -OH group. For CA, we selected H7a and H7a' from -OH groups; these are the hydrogens with the lower D_0 value (Fig. 1). For CAPE, we selected H7a from the -OH group. Our results were compared with experimental results. Experimental previous work shows that CAPE [60], CA [61, 62], and curcumin [63] are not ionized at physiological pH 7.4. The experimental pK_a reported for curcumin is 8.38 ± 0.04 [63]. It is known that cycle A, for the proton exchange scheme, is not very accurate, but our results agree with experimental results, which is enough for this work's scope.

Variation in global descriptors

To study the electron transfer between AR and FR, we analyzed the global chemical reactivity descriptors of CAPE, CA, curcumin, Vit A, and Vit E. We found that CDK, CKE, CA, and CAPE behave as antireductants while vitamins as antioxidants. Furthermore, we found that all of them are more reactive in water than in pentyl ethanoate (Fig. 2), where we present the values of the global chemical reactivity descriptors. In Fig. 2a and c, we see those molecules with the lower values of I have the following order Vit A < Vit E < CKE < CAPE < CDK < CA; a lower I means a higher probability of losing an electron, i.e., Vit A and Vit E have a higher likelihood of donating an electron to a FR. We saw that the molecules with higher values of A might be arranged in the following order CKE > CDK > CAPE > CA > Vit A > Vit E; a higher value of A means a higher probability of gaining an electron from a FR, i.e., CKE, CDK, and CAPE can more easily accept an electron from a FR.

On the other hand, molecules with the lower values of η follow the order CKE < Vit A < CDK < CAPE < Vit E < CA; a lower value of η means higher reactivity (higher values of η for more stable molecules). Additionally, the molecules with a lower value of χ are Vit A and Vit E; they may share electrons more easily. In Fig. 2b, we see that the molecules with the lower values of ω have the following order Vit E < Vit A < CA < CDK < CKE < CAPE; molecules with a lower value of ω are expected to be efficient for scavenging free radicals via electron transfer, then Vit A and Vit E should be more reactive. Also, we see those molecules with the highest values of ω^+ have the following order CKE > CDK > CAPE > Vit A > CA > Vit E; a higher value of ω^+ means a higher probability to accept charge from a FR, then CKE and CDK should accept charge more easily. Moreover, we see that the molecules with the lower value of ω^- follow the order Vit E < Vit A < CA < CAPE < CDK < CKE; the lower value of ω^- means higher probability to donate charge to a FR, then Vit E and Vit A would donate charge more easily to a FR. This trend was observed in the pentyl ethanoate phase. We observe that there are no differences in behavior between the different conformers of each molecule.

Solvation energy and log *P*

Calculations of ΔG°_{solv} and log P help to assess the solubility of a molecule in each solvent. We found that CKE, CDK, and CAPE are lipophilic molecules according to their log P

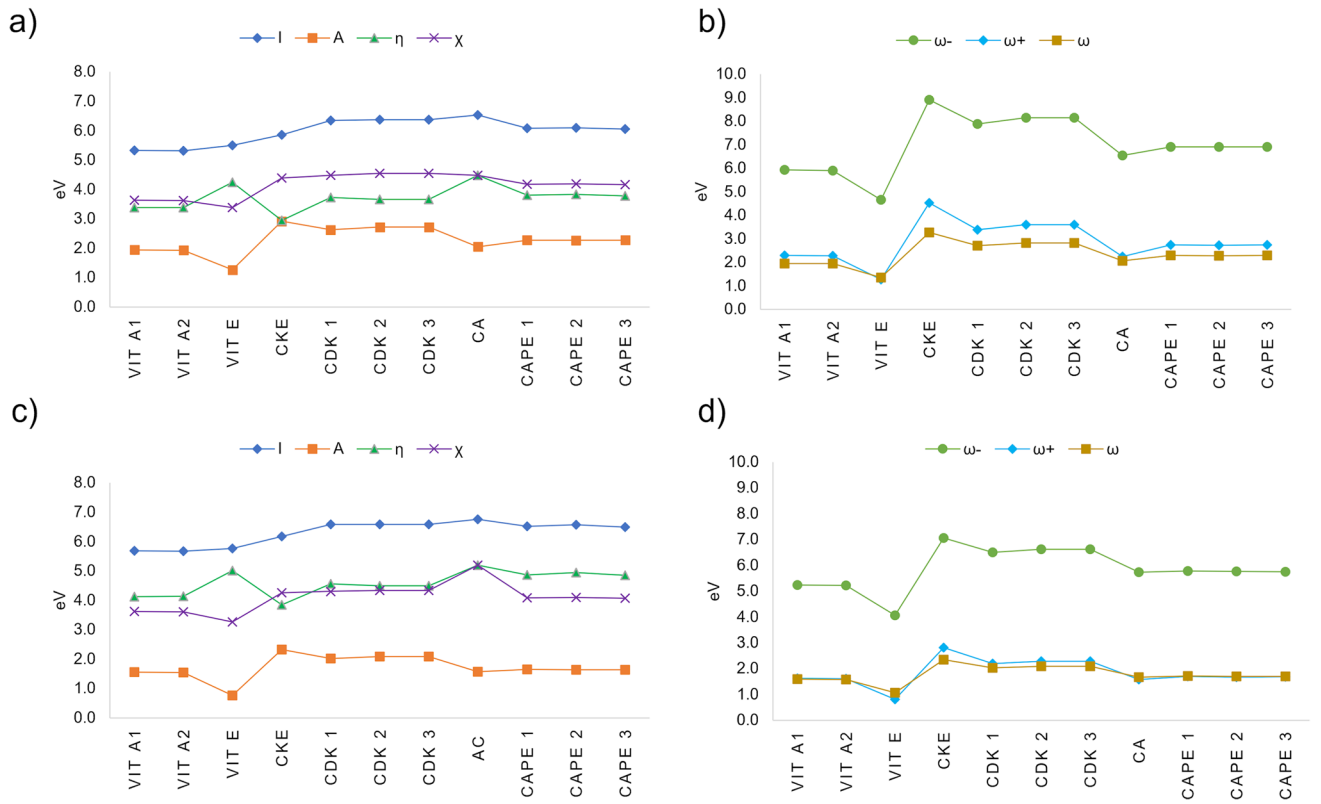

Fig. 2 Global descriptors computed for CAPE, CA, CDK, CKE, Vit A, and Vit E at M06-2X/6–31 + G* level of theory. **a** and **b** show values in water and **c** and **d** show values in pentyl ethanoate

Table 3 Log *P* value and Solvation free energy (ΔG°_{solv}) values in water ($\Delta G_{solv,w}$) and pentyl ethanoate ($\Delta G_{solv,p}$) of each molecule at the M06-2X/6–31 + G*/SMD level of theory

Molecule	Log *P*	$\Delta G_{solv,w}$(kcal/mol)	$\Delta G_{solv,p}$(kcal/mol)
Vit C	− 2.85	− 22.98	− 13.56
Vit A	4.69	− 6.82	− 14.03
Vit E	9.8	− 4.86	− 15.18
CKE	0.89	− 16.57	− 18.18
CDK	2.52	− 17.93	− 18.83
CA	1.78	− 49.34	− 32.44
CAPE	2.75	− 15.32	− 16.70

and ΔG°_{solv} values; see Table 3. We compare the results of CDK, CKE, CAPE, and CA with Vit A and Vit E. It is clear that Vit A and Vit E are lipophilic, in agreement with the literature [64, 65]. Hence, our methodology can reproduce the known experimental results. We added Vit C, a known hydrophilic molecule, as control. Our results also show that Vit C is hydrophilic. Thus, CDK, CKE, and CAPE are more energetically stable in pentyl ethanoate solvent than in water, but they are also stable. There is only a small difference between energies in water and pentyl ethanoate. This little difference would indicate the capacity to cross the cell membrane given this amphiphilic character. On the other hand, for CA, its log *P* value shows CA as a lipophilic molecule, while its ΔG°_{solv} shows CA as hydrophilic. However, the difference in energies is small. According to its computed pK_a value, CA is mostly lipophilic, in agreement with the known fact that phenolic compounds have low solubility in water.

Bioavailability and toxicity

To investigate the use of our molecules as drugs with potential therapeutic applications, we consider several molecular descriptors from the Lipinski's rules, Ghose's rules, and Veber's criteria and descriptors for toxicity (Table 4). As a result, CKE, CDK, and CAPE do not violate more than one of these rules; then, they are predicted to have good bioavailability. It is important to note that these rules are empirical, so they are a guideline, not rigorous law. On the other hand, we consider the toxicity descriptors, the lower value of M, and the larger value of LD_{50} means low toxicity for molecules. Henceforth, CDK, CKE, CA, and CAPE are not toxic due to a lower and negative value of M and a larger

Table 4 Molecular descriptors (log *P*, PSA, HBD, HBA, MW, nAtom, nRB, and AMR) from Lipinski's rules, Ghose's rules, and Veber's criteria and descriptors for toxicity, oral rat 50% lethal dose (LD_{50}), and Ames mutagenicity (M) for CAPE, CA, CDK, CKE, and controls Vit A, Vit E, Vit C, DDT, and pipobroman

Molecule	Log *P*	PSA	HBD	HBA	MW	nAtom	nRB	AMR	LD_{50}	M
Vit A	4.69	20.158	1	1	286.46	51	5	96.76	1495.040	0.55 (+)
Vit E	9.80	22.263	1	2	428.70	79	12	130.27	5742.540	0.08 (-)
CKE	0.89	75.675	3	6	368.39	47	7	113.73	987.190	0.05 (-)
CDK	2.52	77.935	2	6	368.39	47	8	111.70	1015.000	0.09 (-)
CA	1.78	183.561	6	12	474.37	52	11	120.05	4466.050	0.19 (-)
CAPE	2.75	57.156	2	4	284.31	37	6	88.38	3611.100	0.06 (-)
Vit C									11,908.53*	0.29 (-)
DDT									87.01*	0 (-)*
Pipobroman									220.06*	1(+)*

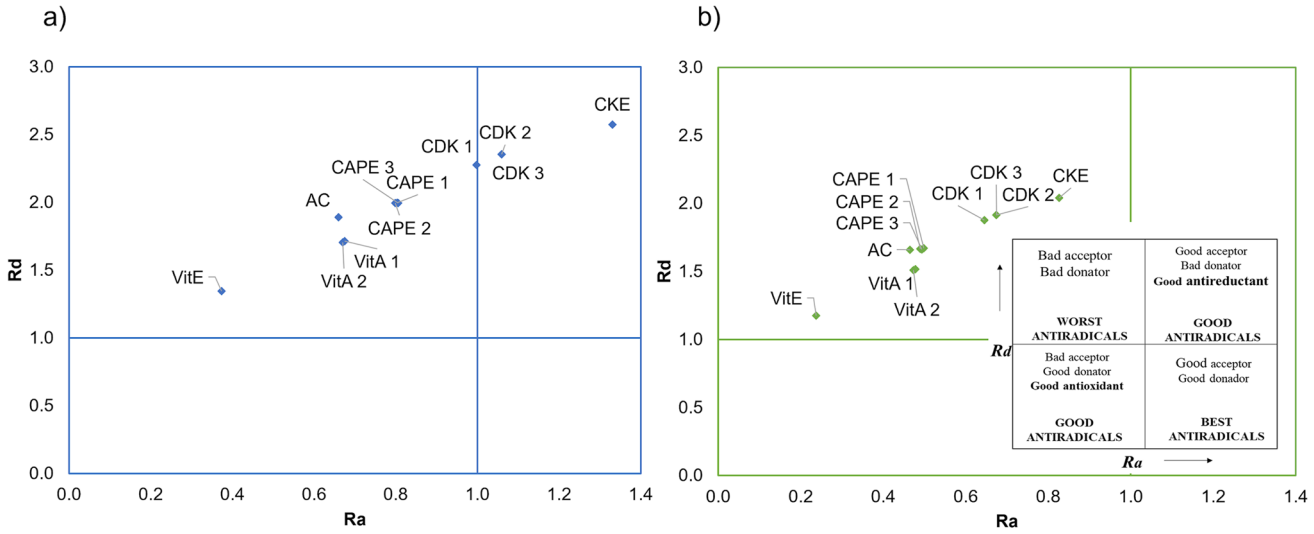

Fig. 3 DAM map of the molecules studied. **a** Molecules in water and **b** molecules in pentyl ethanoate

value of LD_{50}. Our results were compared with the values of the non-toxic Vit C and the toxic DDT and pipobroman, values in Table 4. Thus, we can confirm that our molecules should be non-toxic. As can be seen, CKE, CDK, and CAPE seem to be the most promising for being further tested as drugs with potential therapeutic use.

Single electron transfer

To evaluate the SET mechanism, we used simple strategies as DAM and FEDAM maps. In the DAM map, we found that CDK and CKE are good antireductants in water, as shown in Fig. 3. CDK and CKE are much

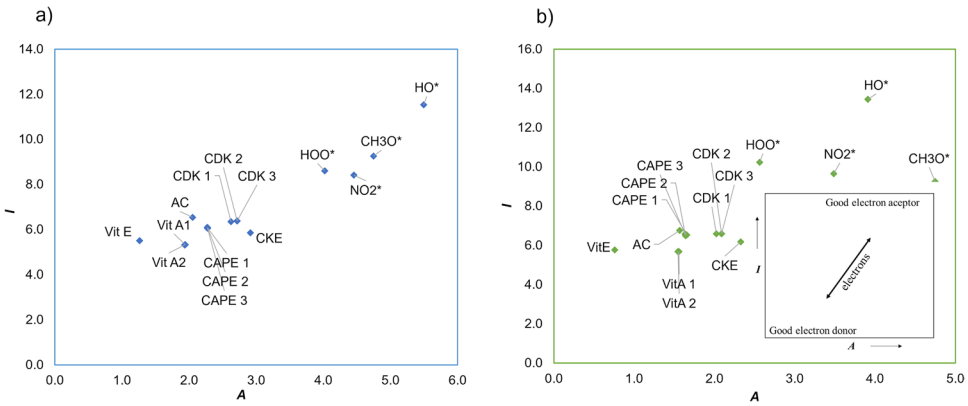

Fig. 4 FEDAM map of the molecules studied. **a** Molecules in water and **b** molecules in pentyl ethanoate

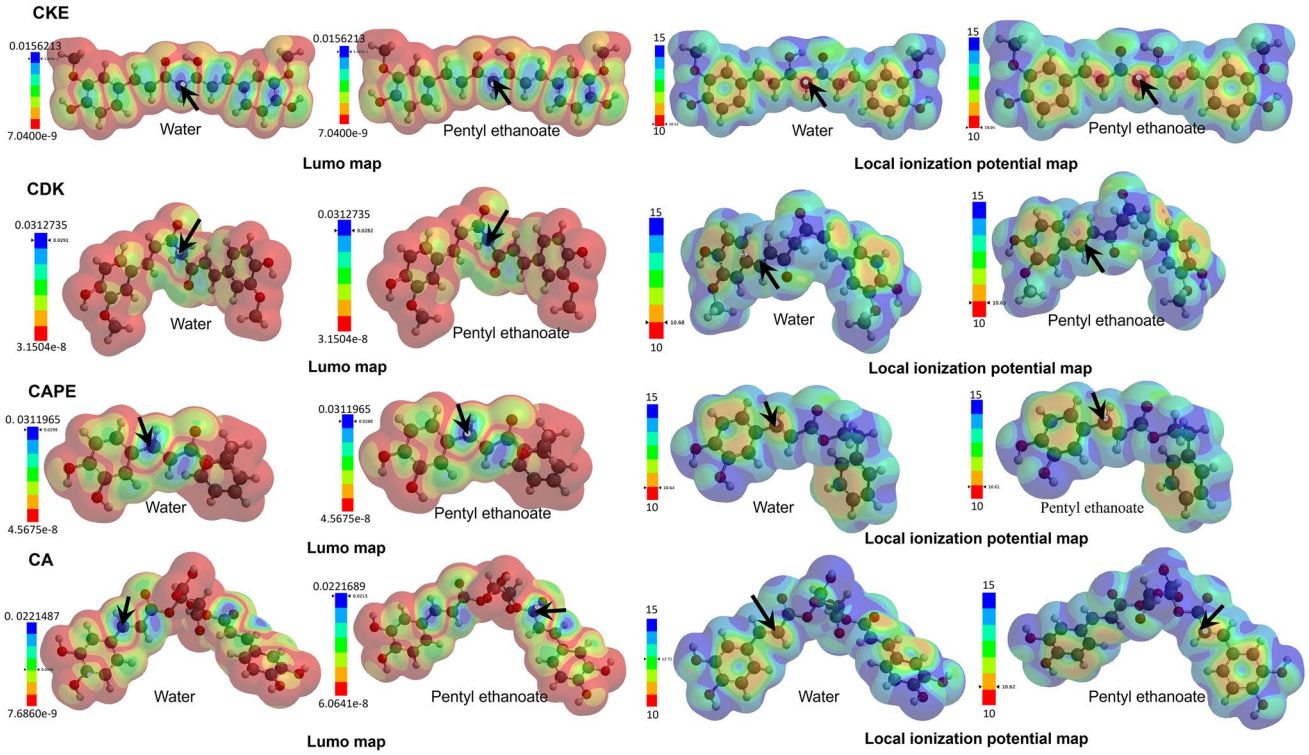

Fig. 5 LUMO map (left) and local ionization potential map (right) for CKE, CDK, CAPE, and CA. Black arrow points to atoms that can accept or donate an electron more readily to a FR. For the LUMO map, blue color identifies atoms that can accept charge easily, while in the local ionization potential map, red color identifies the atom that can donate charge more easily

weaker electron donors and better electron acceptors. Therefore, CDK and CKE have better antiradical properties in water than Vit A and Vit E. This result may be due to their phenolic structure. Hence, CKE and CDK have more -OH groups than Vit A and Vit E. However, CDK and CKE have fewer -OH groups than CA, but CA has difficulties donating or accepting electrons, as we saw in the global chemical reactivity descriptors. On the other hand, in Fig. 4, we used the FEDAM map to evaluate fast transfer processes and analyze the feasibility of donating or accepting an electron from FR. In this map, the molecules down and left will transfer electrons more easily to the FR molecules located up and right, and molecules near FR can accept electrons from FR. CDK and CKE are up and right to $HOO^{\cdot}$; they have higher A than the other molecules in both solvents. CDK and CKE are expected to be able to accept an electron from $HOO^{\cdot}$. Consequently, only CDK and CKE would undergo the SET mechanism and mostly in water.

To identify which atoms can more easily donate or accept charge from a FR, we propose to use the LUMO map and local ionization potential map (local chemical descriptors). The LUMO map shows the absolute value of the LUMO mapped onto an electron density isosurface with a color code. Blue indicates a high concentration of the LUMO, while red suggests low LUMO. With high values in the LUMO map, a nucleophilic attack is predicted to occur more likely; then, atoms with blue color can more easily accept an electron from a FR molecule. Local ionization potential map indicates the ease or difficulty for local electron removal, and this map shows the value of the local ionization potential mapped onto an electron density isosurface with a color code. Red indicates low ionization potential, while blue indicates high ionization potential. Therefore, atoms in red can more easily donate an electron to a FR molecule. In this sense, in Fig. 5, we can see the atoms, marked with a black arrow, in every molecule that can donate or accept an electron from a FR. In both solvents, we can see the same atoms behave similarly. From the values of the global chemical reactivity descriptors, we can see that CDK, CKE, CAPE, and CA have difficulties donating an electron; thus, acceptance of electrons occurs. Hence, the atoms shown in the LUMO map with blue color can accept an electron from a FR more readily. Electrophilic or nucleophilic agents can easily attack these sites in real biological systems. The results for the vitamins are in the supporting information (Fig. S4).

Table 5 Atoms studied in hydrogen atom transfer mechanism for each molecule This table shows the number of reactive atoms within each FR; in parenthesis, the more exergonic reactions are shown

Molecule	# atoms	Water				Pentyl ethanoate			
		$OH^{\cdot}$	$CH_3O^{\cdot}$	$HOO^{\cdot}$	$NO_2^{\cdot}$	$OH^{\cdot}$	$CH_3O^{\cdot}$	$HOO^{\cdot}$,	$NO_2^{\cdot}$
CKE	8	**8 (1°)**	**2 (2°)**	**2 (3°)**	**2 (4°)**	5 (1°)	2 (2°)	2 (3°)	–
CDK	4/8*	**4/8* (1°)**	**3/6* (2°)**	**1/2* (3°)**	**–**	4/8* (1°)	2/4* (2°)	1/2* (3°)	–
CA	8/16*	6/12* (1°)	2/2* (2°)	2/4* (3°)	2/4* (4°)	**8/16* (1°)**	**2/4* (2°)**	**2/4* (3°)**	**2/4* (4°)**
CAPE	9	**9 (1°)**	**5 (2°)**	**2 (3°)**	**2 (4°)**	9 (1°)	3 (2°)	1 (3°)	1 (4°)

*Total number of atoms

() in parenthesis the order of exergonicity

– not exergonic reaction

Hydrogen atom transfer

Furthermore, we evaluated the hydrogen atom transfer mechanism, where we found that CA and CAPE should be good antiradicals following this mechanism. We calculated the dissociation energy of one hydrogen atom (D_0) shown in Fig. 1 and adiabatic Gibbs free energy (ΔG) for the FR: $OH^{\cdot}$, $NO_2^{\cdot}$, $HOO^{\cdot}$, and $CH_3O^{\cdot}$. To find the best antiradical following this mechanism, we must consider the number of reactive hydrogen atoms in the given molecule and the Gibbs free energies for the hydrogen atom transfer. Negative values for Gibbs free energies indicate that the reaction is exergonic and energetically possible. The dissociated hydrogen atom which produces exergonic reactions is considered an active hydrogen. Molecules with many active hydrogen atoms are more reactive; therefore, they should behave as better antiradicals. The total number of active hydrogens is shown in Table 5 (see supporting information Tables S1-S4 for more detailed information). We studied the bond dissociation energy of the active hydrogens of each molecule shown in blue in Fig. 1. For example, for CKE, we studied eight bonds and for CAPE, nine bonds. On the other hand, we only considered the side of the molecule of CDK and CA that has symmetry. Thus, for CDK, we studied four bonds, but it has eight bonds susceptible to donate H, while for CA, we reviewed eight, but it has 16 bonds in total. These can be seen in Fig. 1.

The more reactive antiradical was found to be CA because it is reactive with all studied FRs in both solvents. However, it is more reactive in pentyl ethanoate than in water, as can be seen in Table S4; we show this result with bold letters in Table 5. Also, CA reacts with all the FR in the order shown in parenthesis. As we can see, the most favorable reaction of CA should be with $OH^{\cdot}$. The second more reactive antiradical is CAPE with nine active hydrogen atoms. CAPE is more reactive in water with all the evaluated FR, especially with $OH^{\cdot}$. The third is CKE and CDK with eight reactive hydrogens; both molecules were more reactive in water. In our previous results, we found that all these molecules are lipophilic; however, they can donate hydrogen atoms more easily in water. This result indicates that they should be able to transfer hydrogen atoms in both solvents. The hydrogen atom that more easily transfers is an acidic hydrogen in all cases.

We also studied the formation of bond hydrogens. A strong intermolecular hydrogen bonding is thermodynamically more favorable; this may cause the highest value of D_0 and ΔG, and in consequence, the lowest antioxidant potential. We found moderate and weak hydrogen bonds in CDK, CKE, and CAPE, as shown in Fig. S5. CKE and CDK have three and two hydrogen bonds, respectively, while CAPE has one. CKE has two weak hydrogen bonds between the -OH groups of the phenol and the methoxy group, and it also has one moderate hydrogen bond in the keto-enol species. CDK has two moderate hydrogen bonds between the -OH groups of the phenol and the methoxy. Finally, CAPE has one moderate hydrogen bond between the -OH groups. These hydrogen bonds may indicate why it is more difficult for CDK and CKE to transfer a hydrogen atom than for CA and CAPE.

Inhibition of xanthine oxidase

XO is an enzyme involved in the catabolism of purines in humans. XO generates $O_2^{\cdot -}$ and H_2O_2 during its mechanism of reaction [66]. Then, XO generates significant amounts of FRs; it represents an important source of free radicals [67]. To inhibit XO activity, we used molecular docking to explore the binding affinity, binding mode, molecular interactions, and inhibition constant of CDK, CKE, CAPE, CA, Vit A, and Vit E. To validate the docking methodology, we computed the RMSD value for bond lengths to assess the overall quality of obtained geometries when compared with a known species; the method is effective if a value of RMSD is smaller than 3.5 Å when comparing the bonds

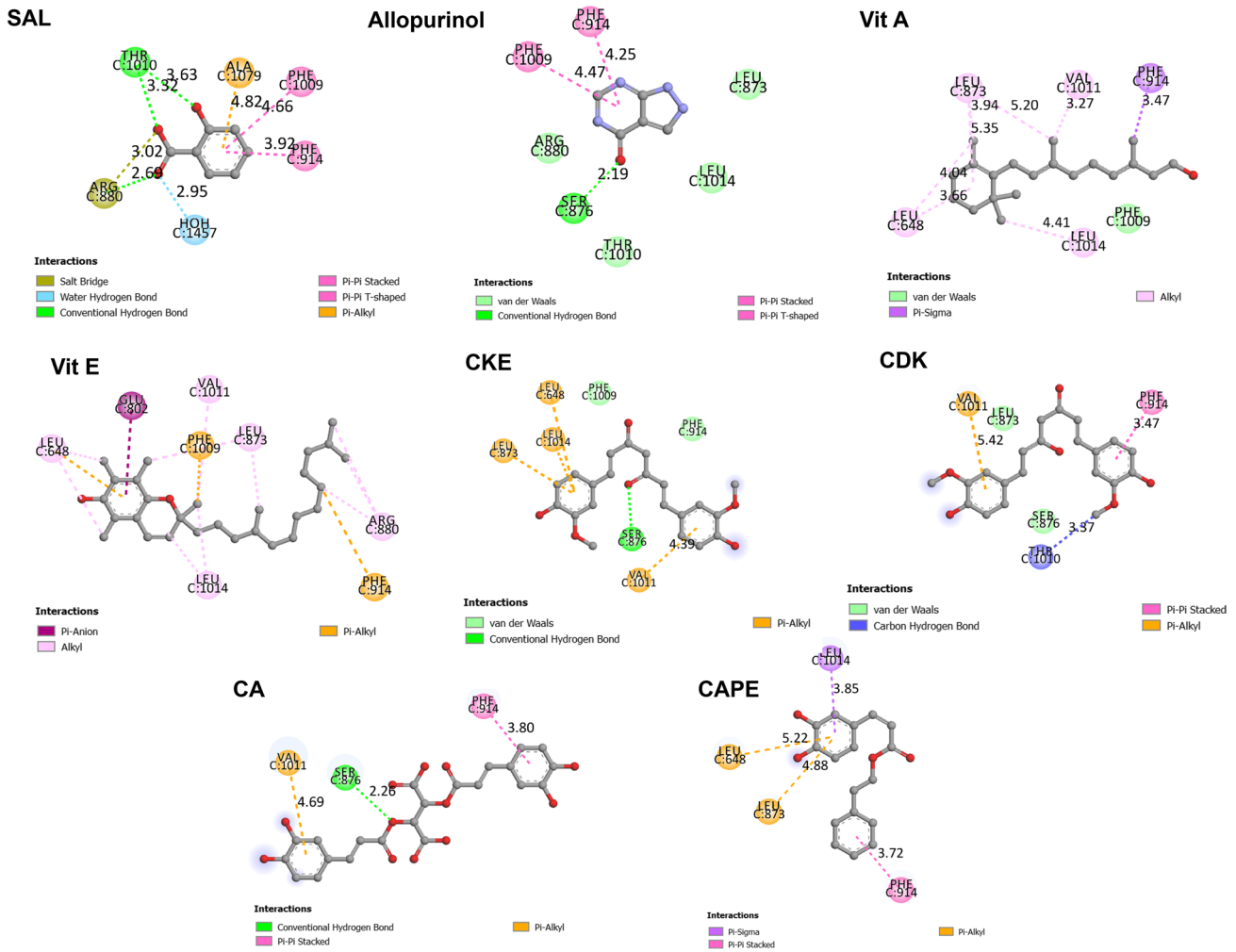

Fig. 6 2D poses and molecular interactions of CKE, CKD, CAPE, CA, and molecules used as controls (SAL and allopurinol) in docking calculations into the active site of XO

in a calculated system with the same bonds in the reference. The docking method validation was done by redocking the natural ligand receptor on the active site, the salicylic acid (SAL). Also, we used the allopurinol molecule, a well-known competitive inhibitor of the XO enzyme [68].

The obtained docking poses for the docked inhibitor were within 1.33 Å for the RMSD of the docked ligand crystal structure. Significant interactions were depicted as hydrogen bonding, $\pi\ \pi$ bonding, and π-alkyl bonding, in Fig. 6. The inhibitors were docked near the binding site; however, CDK, CKE, CAPE, CA, and vitamins A and E were not able to interact directly with the Mo cofactor in XO. In Fig. 6, it is noteworthy that SAL and allopurinol exhibit strong molecular interactions with XO; the binding energy and ligand efficiency reflect this. A high value of binding energy and ligand efficiency means a stronger interaction with the target. Ligand efficiency is used to compare the activity of different molecules regardless of different sizes. On the other hand, the inhibition constant, K_i, indicates how potent an inhibitor is; it is the concentration required to produce half-maximum inhibition.

It is noteworthy that SAL and allopurinol, according to their binding energy and ligand efficiency, inhibit XO more efficiently than our molecules; see Table 6. Also, we note that Vit A, CKE, and CA have high values of K_i; this means that high quantities of these molecules are necessary to inhibit the activity of XO. On the other hand, the molecules with a low value of K_i and high value of binding energy and ligand efficiency are the best to inhibit XO. CDK and CAPE could inhibit XO; however, they are not better than SAL and allopurinol.

Conclusions

The antiradical properties of CDK, CKE, CAPE, and CA were investigated at the M06-2X/6–31 + G* DFT level of theory. This level was selected after we performed a benchmark

Table 6 Binding energy, ligand efficiency, and K_i values for each molecule

Molecule	Binding energy (kcal/mol)	Ligand efficiency (kcal/mol)	Inhibition constant, K_i (μM)
Vit A	−8.22	−0.39	941.04
Vit E	−3.98	−0.13	1.21
CKE	−5.40	−0.20	110.44
CDK	−7.25	−0.27	4.84
CA	−5.12	−0.15	177.92
CAPE	−7.26	−0.35	4.79
SAL	−7.54	−0.75	2.96
Allopurinol	−8.13	−0.81	1.10

study comparing results from several levels of theory with the experimental value of the vertical ionization energy of vitamin A as reference. Our results show that CDK, CKE, CAPE, and CA should behave as good antiradicals. We find that these molecules have good antiradical properties such as good bioavailability and low toxicity. Some properties were evaluated to provide a good quantitative characterization and description of the most plausible mechanisms of action of the suggested antiradicals. First, the pK_a was estimated. We found that at physiological pH, all molecules are in neutral form; in consequence, neutral forms were the only studied since they are the most important species for a biological study. Thereafter, the solubility of these molecules was estimated computing the log P and ΔG°_{solv}. Our results show that CKE, CDK, and CAPE are mainly lipophilic molecules. Our methodology was validated with the vitamin A and vitamin E (lipophilic molecules) and vitamin C (hydrophilic molecule) used as references or controls. Furthermore, the ADME properties and toxicity were assessed by calculating the Lipinski's rules, Ghose's rules, Veber's criteria, LD_{50}, and mutagenicity. Our results indicate that CKE, CDK, and CAPE should be useful drugs with potential therapeutic use due to the excellent values obtained for these properties and their non-toxic nature. Finally, we evaluated some possible antiradical mechanisms of action: SET, HAT, and XO inhibition.

For the study of electron transfer, several global chemical reactivity descriptors were computed; and we found that CDK, CKE, CA, and CAPE behave as antireductants while vitamin A and E as antioxidants. In the study of the SET mechanism, we used two simple graphical techniques to accommodate in a simple manner our numerical results: the DAM map and FEDAM map. These devices allow a rapid quantitative characterization of the antiradical properties of the studied molecules. CDK and CKE are found to be weaker electron donors and better electron acceptors; they are good antireductants according to the SET mechanism. Also, we noticed that CDK and CKE can accept an electron from $^{\bullet}$OOH. However, this mechanism implies a higher energy cost.

On the other hand, the HAT mechanism was more energetically favorable. The best antiradicals turned out to react following the HAT mechanism, CA, and CAPE with more active hydrogen atoms to be transferred to the free radicals. CA and CAPE were found to be the best antiradicals to react with $OH^{\bullet}$. Although the best molecules to inhibit XO are predicted to be CDK and CAPE, they are not better than the controls SAL and allopurinol.

Our DFT global descriptors of reactivity results can anticipate other mechanisms of action, not studied here, such as sequential electron-proton transfer (SET-PT). The obtained high values of I indicate that our molecules will hardly present SET-PT mechanisms in both the physiological and lipophilic medium. The same should happen with the sequential proton loss hydrogen atom transfer (SPLHAT) mechanism. Consequently, this research may motivate further studies on the subject, to include these other mechanisms not studied so far. In conclusion, we suggest that CDK, CKE, CAPE, and CA may have a potential role as protectors against oxidative stress scavengers and the associated health issues.

Supplementary Information The online version contains supplementary material available at https://doi.org/10.1007/s00894-022-05056-4.

Acknowledgements The Guanajuato National Laboratory (CONACYT 1237332) is acknowledged for use of supercomputing resources.

Author contribution Brenda Manzanilla: Performed DFT calculations, formal analysis, visualization, and writing the manuscript. Juvencio Robles: General discussion, integration, resources, supervision, coordination, and writing the manuscript. All authors read and approved the final manuscript.

Funding BM acknowledges support from CONACYT for a Ph.D. scholarship (580068/296892). JR gratefully acknowledges funding from University of Guanajuato DAIP-*Convocatoria Institucional de Investigación Científica* 2018, project No. 268.

Data availability All data generated or analyzed during this study are included in this article and in the Supplementary Information (SI) submitted to this journal.

Code availability Not applicable.

Declarations

Competing interests The authors declare no competing interests.

References

1. Phaniendra A, Jestadi DB, Periyasamy L (2015) Free radicals: properties, sources, targets, and their implication in various diseases. Indian J Clin Biochem 30:11–26. https://doi.org/10.1007/s12291-014-0446-0

2. Sies H (2019) Oxidative stress. Stress: Physiology, Biochemistry, and Pathology 153–163. https://doi.org/10.1016/B978-0-12-813146-6.00013-8
3. Oroian M, Escriche I (2015) Antioxidants: characterization, natural sources, extraction and analysis. Food Res Int 74:10–36. https://doi.org/10.1016/j.foodres.2015.04.018
4. Chaiyasit W, Elias RJ, McClements DJ, Decker EA (2007) Role of physical structures in bulk oils on lipid oxidation. Crit Rev Food Sci Nutr 47:299–317. https://doi.org/10.1080/10408390600754248
5. A Galano J Raúl Alvarez-Idaboy 2019 Computational strategies for predicting free radical scavengers' protection against oxidative stress: where are we and what might follow? Int J Quantum Chem 119. https://doi.org/10.1002/qua.25665
6. Pisoschi AM, Pop A (2015) The role of antioxidants in the chemistry of oxidative stress: a review. Eur J Med Chem 97:55–74. https://doi.org/10.1016/j.ejmech.2015.04.040
7. Ehrlich K, Ehrlich K, Viirlaid S et al (2007) Design, synthesis and properties of novel powerful antioxidants, glutathione analogues. Free Radical Res 41:779–787. https://doi.org/10.1080/10715760701348611
8. Hussain HH, Babic G, Durst T et al (2003) Development of Novel Antioxidants: design, Synthesis, and Reactivity. J Org Chem 68:7023–7032. https://doi.org/10.1021/jo0301090
9. Zhang H-Y, Yang D-P, Tang G-Y (2006) Multipotent antioxidants: from screening to design. Drug Discovery Today 11:749–754. https://doi.org/10.1016/j.drudis.2006.06.007
10. Reina M, Castañeda-Arriaga R, Perez-Gonzalez A, et al (2018) A computer-assisted systematic search for melatonin derivatives with high potential as antioxidants. Melatonin Research 1:27–58. https://doi.org/10.32794/mr11250003
11. Ji H-F, Tang G-Y, Zhang H-Y (2005) A theoretical study on the structure–activity relationships of metabolites of folates as antioxidants and its implications for rational design of antioxidants. Bioorg Med Chem 13:1031–1036. https://doi.org/10.1016/j.bmc.2004.11.047
12. Zhang H-Y, Sun Y-M, Wang X-L (2003) Substituent effects on OH bond dissociation enthalpies and ionization potentials of catechols: a DFT study and its implications in the rational design of phenolic antioxidants and elucidation of structure–activity relationships for flavonoid antioxidants. Chemistry – A European Journal 9:502–508. https://doi.org/10.1002/chem.200390052
13. Castañeda-Arriaga R, Pérez-González A, Reina M, Galano A (2020) Computer-designed melatonin derivatives: potent peroxyl radical scavengers with no pro-oxidant behavior. Theoret Chem Acc 139:1–12. https://doi.org/10.1007/s00214-020-02641-9
14. Martínez A, Melendez-Martínez AJ (2016) Lycopene, oxidative cleavage derivatives and antiradical activity. Comput Theor Chem 1077:92–98. https://doi.org/10.1016/j.comptc.2015.11.001
15. Y Romero A Martínez 2015 Antiradical capacity of ommochromes J Mol Model 21. https://doi.org/10.1007/s00894-015-2773-3
16. Reina M, Martínez A (2015) Silybin and 2,3-Dehydrosilybin flavonolignans as free radical scavengers. J Phys Chem B 119:11597–11606. https://doi.org/10.1021/acs.jpcb.5b06448
17. Galano A, Álvarez-Diduk R, Ramírez-Silva MT et al (2009) Role of the reacting free radicals on the antioxidant mechanism of curcumin. Chem Phys 363:13–23. https://doi.org/10.1016/j.chemphys.2009.07.003
18. TEA Ardjani JR Alvarez-Idaboy 2018 Radical scavenging activity of ascorbic acid analogs: kinetics and mechanisms Theoret Chem Acc 137. https://doi.org/10.1007/s00214-018-2252-x
19. Dao DQ, Ngo TC, Thong NM, Nam PC (2017) Is Vitamin A an antioxidant or a pro-oxidant? J Phys Chem B 121:9348–9357. https://doi.org/10.1021/acs.jpcb.7b07065
20. Ak T, Gülçin I (2008) Antioxidant and radical scavenging properties of curcumin. Chem Biol Interact 174:27–37. https://doi.org/10.1016/j.cbi.2008.05.003
21. Lee J, Scagel CF (2009) Chicoric acid found in basil (Ocimum basilicum L.) leaves. Food Chem 115:650–656. https://doi.org/10.1016/j.foodchem.2008.12.075
22. Zhu X, Huang F, Xiang X et al (2018) Evaluation of the potential of chicoric acid as a natural food antioxidant. Exp Ther Med 16:351–3657. https://doi.org/10.3892/etm.2018.6596
23. Carreño AL, Alday E, Quintero J et al (2017) Protective effect of Caffeic Acid Phenethyl Ester (CAPE) against oxidative stress. J Funct Foods 29:178–184. https://doi.org/10.1016/j.jff.2016.12.008
24. Geerlings P, De Proft F, Langenaeker W (2003) Conceptual density functional theory. Chem Rev 103:1793–1874. https://doi.org/10.1021/cr990029p
25. Chung HY, Baek BS, Song SH et al (1997) Xanthine dehydrogenase/xanthine oxidase and oxidative stress. Age 20:127–140. https://doi.org/10.1007/s11357-997-0012-2
26. Frisch MJ, Trucks GW, Schlegel HB, et al (2010) Gaussian 09. Revision C.01. Gaussian 09. Revision C.01, Gaussian, Inc, Wallingford CT
27. Katsumata S, Ikehata N (2001) HeI photoelectron spectroscopic study of vitamin A and its derivatives. J Electron Spectrosc Relat Phenom 107:139–145. https://doi.org/10.1016/S0368-2048(00)00097-9
28. Marenich AV, Cramer CJ, Truhlar DG (2009) Universal solvation model based on solute electron density and on a continuum model of the solvent defined by the bulk dielectric constant and atomic surface tensions. J Phys Chem B 113:6378–6396. https://doi.org/10.1021/jp810292n
29. Spartan'08, (2008) Wavefunction, Inc., 18401 Von Karman Ave., Suite 435, Irvine, CA 92612, USA
30. Halgren TA (1996) Merck molecular force field I Basis, form, scope, parameterization, and performance of MMFF94. J Comput Chem 17:490–519. https://doi.org/10.1002/(SICI)1096-987X(199604)17:5/6%3c490::AID-JCC1%3e3.0.CO;2-P
31. Halgren TA (1996) Merck molecular force field. II. MMFF94 van der Waals and electrostatic parameters for intermolecular interactions. J Comput Chem 17:520–552. https://doi.org/10.1002/(SICI)1096-987X(199604)17:5/6%3c520::AID-JCC2%3e3.0.CO;2-W
32. Halgren TA (1996) Merck molecular force field. III. Molecular geometries and vibrational frequencies for MMFF94. J Comput Chem 17:553–586. https://doi.org/10.1002/(SICI)1096-987X(199604)17:5/6%3c553::AID-JCC3%3e3.0.CO;2-T
33. Halgren TA, Nachbar RB (1996) Merck molecular force field. IV. conformational energies and geometries for MMFF94. J Comput Chem 17:587–615. https://doi.org/10.1002/(SICI)1096-987X(199604)17:5/6%3c587::AID-JCC4%3e3.0.CO;2-Q
34. Ho J, Coote ML (2009) A universal approach for continuum solvent pKa calculations: Are we there yet? Theoret Chem Acc 125:3–21. https://doi.org/10.1007/s00214-009-0667-0
35. Parr RG, Donnelly RA, Levy M, Palke WE (1978) Electronegativity: the density functional viewpoint. J Chem Phys 68:3801–3807. https://doi.org/10.1063/1.436185
36. Janak JF (1978) Proof that $\partial E/\partial ni = \varepsilon$ in density-functional theory. Phys Rev B 18:7165–7168. https://doi.org/10.1103/PhysRevB.18.7165
37. Casida ME (1999) Correlated optimized effective-potential treatment of the derivative discontinuity and of the highest occupied Kohn-Sham eigenvalue: A Janak-type theorem for the optimized effective-potential model. Phys Rev B 59:4694–4698. https://doi.org/10.1103/PhysRevB.59.4694

38. Parr RG, Pearson RG (1983) Absolute hardness: companion parameter to absolute electronegativity. J Am Chem Soc 105:7512–7516. https://doi.org/10.1021/ja00364a005
39. Yang W, Parr RG (1985) Hardness, softness, and the fukui function in the electronic theory of metals and catalysis. Proc Natl Acad Sci 82:6723–6726. https://doi.org/10.1073/pnas.82.20.6723
40. Parr RG, Yang W (1984) Density functional approach to the frontier-electron theory of chemical reactivity. J Am Chem Soc 106:4049–4050. https://doi.org/10.1021/ja00326a036
41. Gázquez JL, Cedillo A, Vela A (2007) Electrodonating and electroaccepting powers. J Phys Chem A 111:1966–1970. https://doi.org/10.1021/jp065459f
42. Duarte Ramos Matos G, Kyu DY, Loeffler HH et al (2017) Approaches for calculating solvation free energies and enthalpies demonstrated with an update of the FreeSolv database. J Chem Eng Data 62:1559–1569. https://doi.org/10.1021/acs.jced.7b00104
43. Leo AJ (1993) Calculating log Poct from structures. Chem Rev 93:1281–1306. https://doi.org/10.1021/cr00020a001
44. Spartan'18, (2018) Wavefunction, Inc., 18401 Von Karman Ave., Suite 435, Irvine, CA 92612, USA
45. Ghose AK, Pritchett A, Crippen GM (1988) Atomic physicochemical parameters for three dimensional structure directed quantitative structure-activity relationships III: Modeling hydrophobic interactions. J Comput Chem 9:80–90. https://doi.org/10.1002/jcc.540090111
46. Lipinski CA, Lombardo F, Dominy BW, Feeney PJ (2001) Experimental and computational approaches to estimate solubility and permeability in drug discovery and development settings. Adv Drug Deliv Rev 46:3–26. https://doi.org/10.1016/s0169-409x(00)00129-0
47. Ghose AK, Viswanadhan VN, Wendoloski JJ (1999) A knowledge-based approach in designing combinatorial or medicinal chemistry libraries for drug discovery 1 A qualitative and quantitative characterization of known drug databases. J Comb Chem 1:55–68. https://doi.org/10.1021/cc9800071
48. Veber DF, Johnson SR, Cheng H-Y et al (2002) Molecular properties that influence the oral bioavailability of drug candidates. J Med Chem 45:2615–2623. https://doi.org/10.1021/jm020017n
49. Gangwal R, Khandelwal K, Kokkula A, et al Drug Likeness Tool (DruLito). http://www.niper.gov.in/pi_dev_tools/DruLiToWeb/DruLiTo_Developers.html. Accessed 1 Jul 2021
50. Young DM (2010) Toxicity Estimation Software Tool (TEST). In: Green Chemistry Networking Forum. https://www.epa.gov/chemical-research/toxicity-estimation-software-tool-test
51. Martínez A, Vargas R, Galano A (2009) What is important to prevent oxidative stress? A theoretical study on electron-transfer reactions between carotenoids and free radicals. J Phys Chem B 113:12113–12120. https://doi.org/10.1021/jp903958h
52. Martínez A, Rodríguez-Girones MA, Barbosa A, Costas M (2008) Donator acceptor map for carotenoids, melatonin and vitamins. J Phys Chem A 112:9037–9042. https://doi.org/10.1021/jp803218e
53. Enroth C, Eger BT, Okamoto K et al (2000) Crystal structures of bovine milk xanthine dehydrogenase and xanthine oxidase: structure-based mechanism of conversion. Proc Natl Acad Sci USA 97:10723–10728. https://doi.org/10.1073/pnas.97.20.10723
54. Morris GM, Huey R, Lindstrom W et al (2009) AutoDock4 and AutoDockTools4: Automated docking with selective receptor flexibility. J Comput Chem 30:2785–2791. https://doi.org/10.1002/jcc.21256
55. Morris GM, Goodsell DS, Halliday RS et al (1998) Automated docking using a Lamarckian genetic algorithm and an empirical binding free energy function. J Comput Chem 19:1639–1662. https://doi.org/10.1002/(SICI)1096-987X(19981115)19:14%3c1639::AID-JCC10%3e3.0.CO;2-B
56. Cao H, Pauff JM, Hille R (2014) X-ray crystal structure of a xanthine oxidase complex with the flavonoid inhibitor quercetin. J Nat Prod 77:1693–1699. https://doi.org/10.1021/np500320g
57. Nobela O, Renslow RS, Thomas DG et al (2018) Efficient discrimination of natural stereoisomers of chicoric acid, an HIV-1 integrase inhibitor. J Photochem Photobiol, B 189:258–266. https://doi.org/10.1016/j.jphotobiol.2018.10.025
58. Singh DK, Jagannathan R, Khandelwal P et al (2013) In situ synthesis and surface functionalization of gold nanoparticles with curcumin and their antioxidant properties: an experimental and density functional theory investigation. Nanoscale 5:1882–1893. https://doi.org/10.1039/C2NR33776B
59. Puglisi A, Giovannini T, Antonov L, Cappelli C (2019) Interplay between conformational and solvent effects in UV-visible absorption spectra: curcumin tautomers as a case study. Phys Chem Chem Phys 21:15504–15514. https://doi.org/10.1039/C9CP00907H
60. Kudugunti SK, Vad NM, Whiteside AJ et al (2010) Biochemical mechanism of caffeic acid phenylethyl ester (CAPE) selective toxicity towards melanoma cell lines. Chem Biol Interact 188:1–14. https://doi.org/10.1016/j.cbi.2010.05.018
61. Thygesen L, Thulin J, Mortensen A et al (2007) Antioxidant activity of cichoric acid and alkamides from Echinacea purpurea, alone and in combination. Food Chem 101:74–81. https://doi.org/10.1016/j.foodchem.2005.11.048
62. Maggini V, De Leo M, Granchi C et al (2019) The influence of Echinacea purpurea leaf microbiota on chicoric acid level. Sci Rep 9:1–11. https://doi.org/10.1038/s41598-019-47329-8
63. Bernabé-Pineda M, Ramírez-Silva MT, Romero-Romo M et al (2004) Determination of acidity constants of curcumin in aqueous solution and apparent rate constant of its decomposition. Spectrochimica Acta - Part A: Molecular and Biomolecular Spectroscopy 60:1091–1097. https://doi.org/10.1016/S1386-1425(03)00342-1
64. Brossaud J, Pallet V, Corcuff J-B (2017) Vitamin A, endocrine tissues and hormones: interplay and interactions. Endocr Connect 6:R121–R130. https://doi.org/10.1530/EC-17-0101
65. Esterbauer H, Rotheneder M, Striegl G et al (1989) Vitamin E and other lipophilic antioxidants protect LDL against oxidation. Lipid / Fett 91:316–324. https://doi.org/10.1002/lipi.19890910805
66. Kelley EE, Khoo NKH, Hundley NJ et al (2010) Hydrogen peroxide is the major oxidant product of xanthine oxidase. Free Radical Biol Med 48:493–498. https://doi.org/10.1016/j.freeradbiomed.2009.11.012
67. Rajendran P, Nandakumar N, Rengarajan T et al (2014) Antioxidants and human diseases. Clin Chim Acta 436:332–347. https://doi.org/10.1016/j.cca.2014.06.004
68. Lin H-C, Tsai S-H, Chen C-S et al (2008) Structure–activity relationship of coumarin derivatives on xanthine oxidase-inhibiting and free radical-scavenging activities. Biochem Pharmacol 75:1416–1425. https://doi.org/10.1016/j.bcp.2007.11.023